

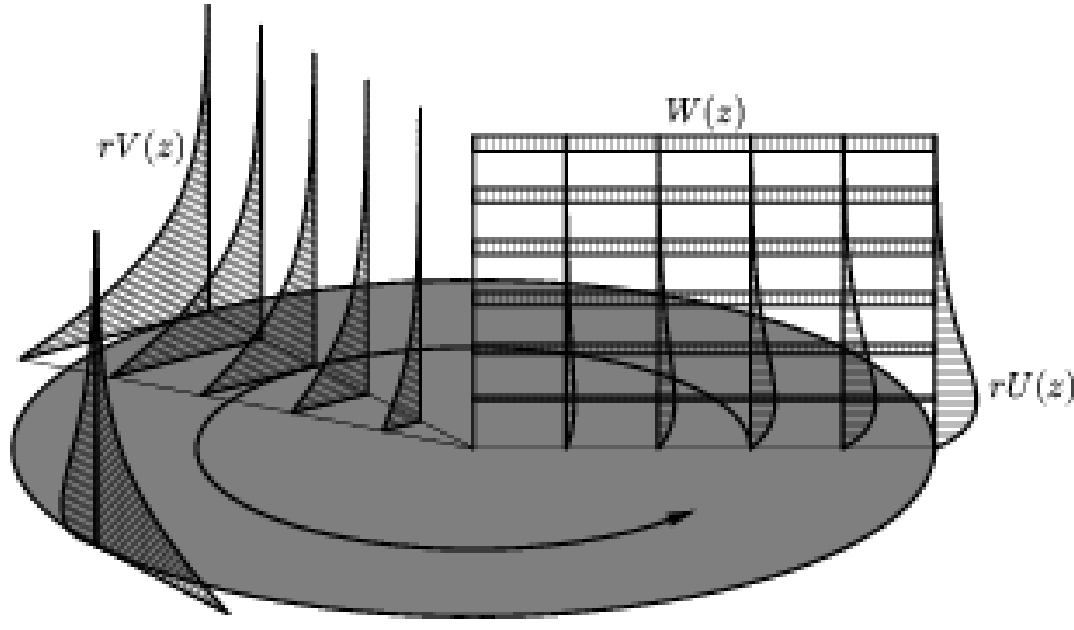
### Rotating Disks $\approx$ Swept Wings

The **steady** rotating disk contains an archetypal model for a **three-dimensional boundary layer**.

Some stability properties are **similar** to those found in the flow over a **swept wing**.

Therefore, any **stabilising techniques** could prove effective in delaying **turbulent onset** on swept wings.

The rotating disk is much **easier** to work with **experimentally** than swept wings.



Steady flow over a disk rotating in a stationary fluid

### Other Points of Interest

- **Reynolds number**  $\equiv$  **local radius** — the further away from the centre, the more unstable the flow.
- The base flow admits an **exact similarity solution** to the Navier-Stokes equations:

$$\mathbf{U}_B = \left( \frac{r}{R}F, \frac{r}{R}G, \frac{1}{R}H \right)$$

where  $(F, G, H)$  are the solutions to a system of ODEs.

### Stabilising Technique - Modulation

We adapt the motion of the disk by way of **periodic modulation** of the surface in the azimuthal plane.

Motivated by **channel flow**, where adding oscillations can be **stabilising** [1].

We alter the **azimuthal boundary condition** of base flow so that:

$$G(z=0, \tau) = 1 + U_w \cos\left(\frac{\varphi}{R}\tau\right) \quad (1)$$

where  $U_w$  gives a measure of the wall velocity and  $\varphi$  the frequency.

### Stability Analysis

- Analyse behaviour of **infinitesimal disturbances** to the flow of the form:

$$\mathbf{U} = \mathbf{U}_B + \epsilon \hat{\mathbf{u}}$$

- Solve Navier-Stokes equations via a velocity-vorticity formulation [2].

#### Floquet theory:

- Take **Floquet mode approximation**

$$p(r, \theta, z, \tau) = \hat{p}(z, \tau) e^{\mu\tau} e^{i(\alpha r + n\theta)} \quad (2)$$

- Decompose  $\hat{p}$  into **harmonics** such that

$$\hat{p} = \sum_{k=-\infty}^{\infty} \hat{p}_n(z) e^{ik\tau}$$

- Gives system of **eigenvalue problems**:

$$\sum_{k=-\infty}^{\infty} \mathcal{L}_k\{\mu, \alpha; n, R, U_w, \varphi\} e^{ik\tau} = 0 \quad (3)$$

#### Direct numerical simulations:

- Retain **full** temporal and radial structure

$$p(r, \theta, z, \tau) = \hat{p}(r, z, \tau) e^{in\theta}$$

- Evolve some pre-determined disturbance via a time-marching procedure.

### Types of Disturbance - Stationary & Impulsive

#### Stationary:

- **Stationary** with respect to disk motion.
  - In Floquet mode expansion (2), set  $\mu = 0$ .
- 
- This is the instability mechanism that is relevant to **swept-wing** flow.

#### Impulsive:

- Prescribe wall motion:
 
$$\zeta(r, \tau) = e^{\lambda r^2} e^{-\sigma \tau^2} \quad (4)$$
 and track development of impulse both temporally and radially.
- This is of interest to more general instability structures, including **transition to turbulence**.

#### Assumptions:

- In order to demonstrate the **stabilising effects** of the modulation on the steady case, we want to keep **close** to the steady case.
- Therefore, we constrain the wall velocity,  $U_w$  in (1) to be:

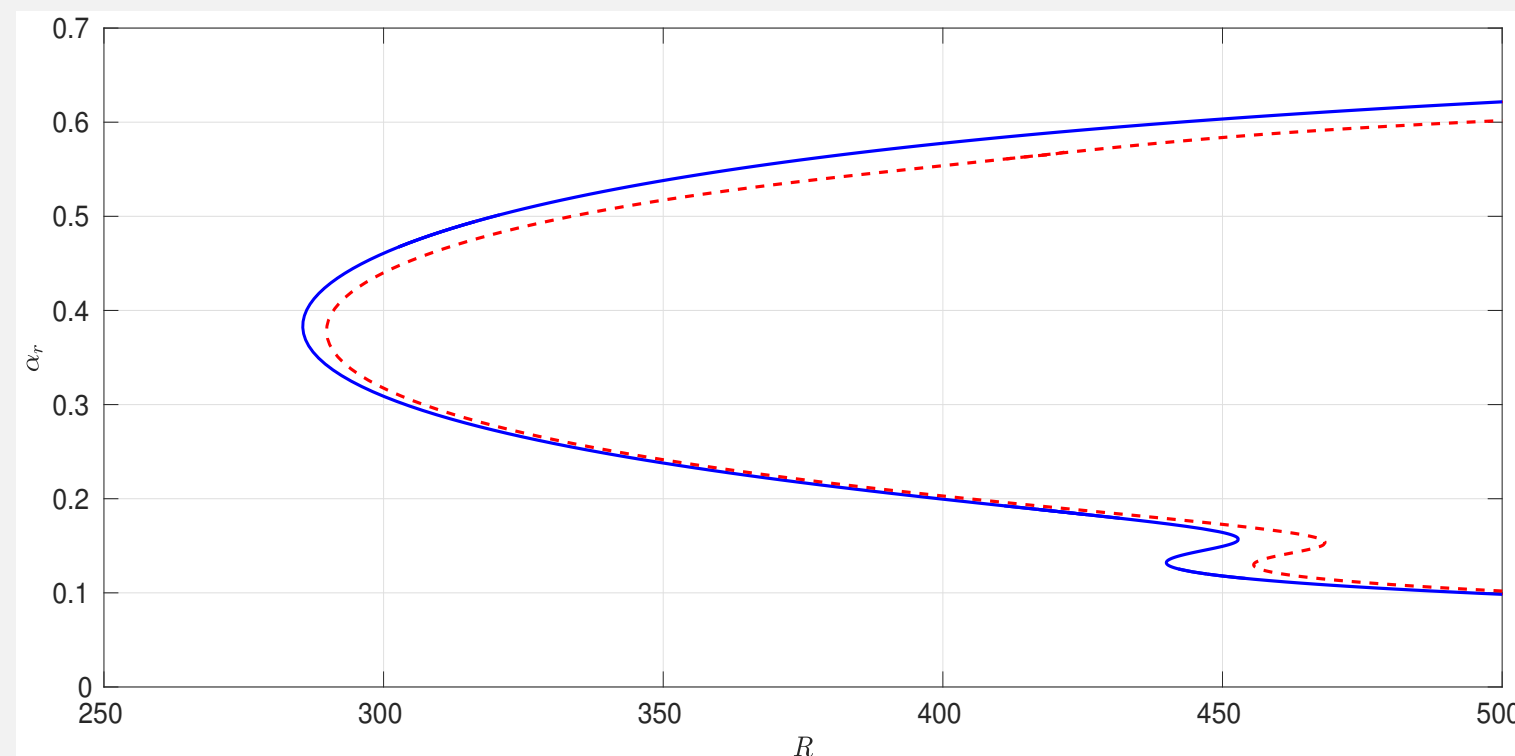
$$U_w \leq 0.2$$

so that the deviation from the steady case is not more than **20%**.

### Stationary Disturbances

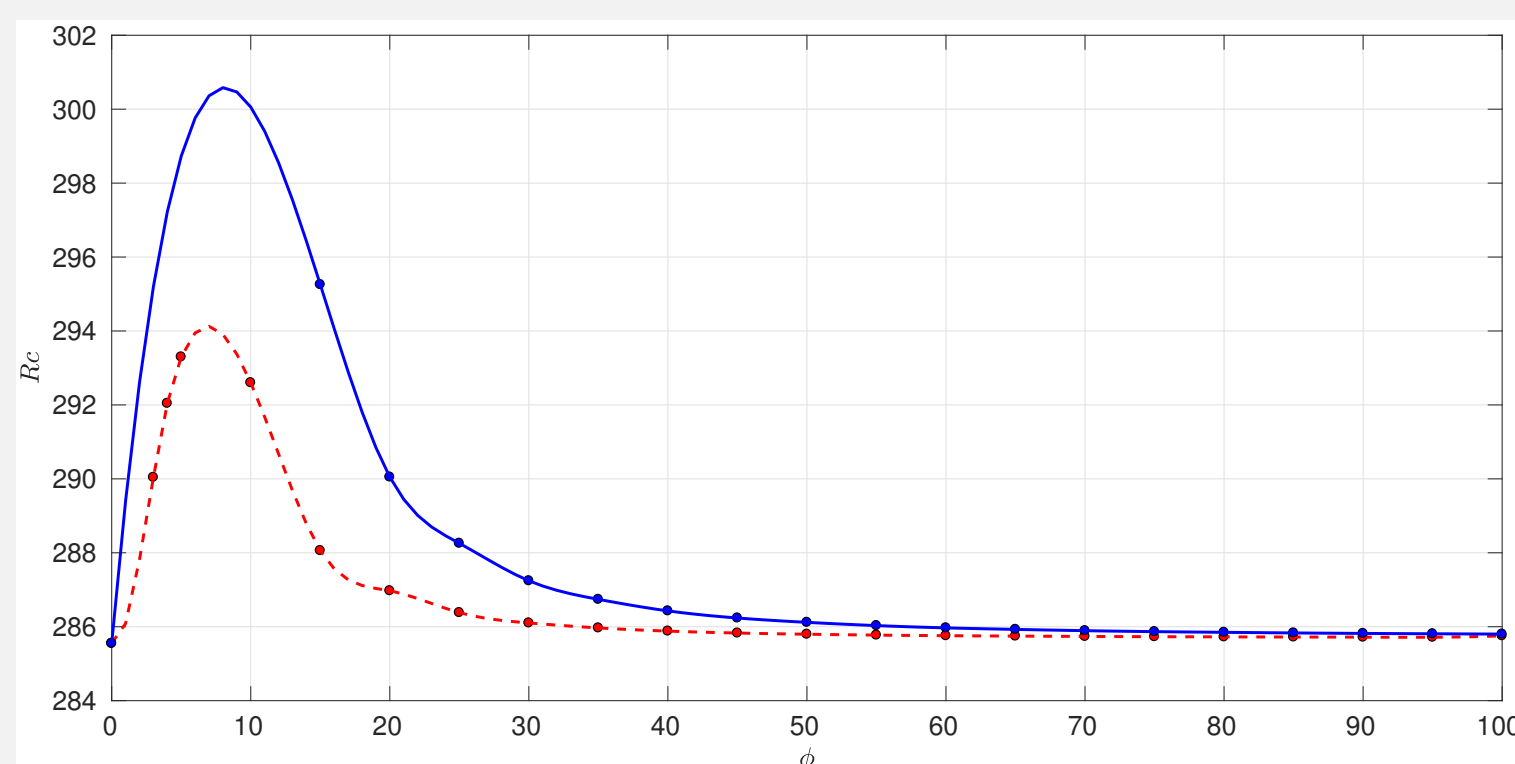
#### Floquet theory:

- Specify  $\mu = 0$  and solve (3) for  $\alpha$ .
- The neutral curve defines the critical value of  $\alpha$  such that  $\Im(\alpha) = 0$ .
- Any parameter values **inside** the curve are **unstable**.
- The **critical Reynolds number**,  $R_c$ , is defined as the smallest Reynolds number for which the flow is unstable. In the steady case,  $R_c \approx 286$ .
- The following figure shows a comparison between the steady neutral curve and that for parameter values  $U_w = 0.2$ ,  $\varphi = 16$  for stationary disturbances.



Comparison between steady (—) and  $U_w = 0.2$ ,  $\varphi = 16$  (---) neutral curves for stationary disturbances.

- The following figure shows a comparison between the critical Reynolds number  $R_c$  for  $U_w \in \{0.1, 0.2\}$  and  $\varphi \in [0, 100]$ .

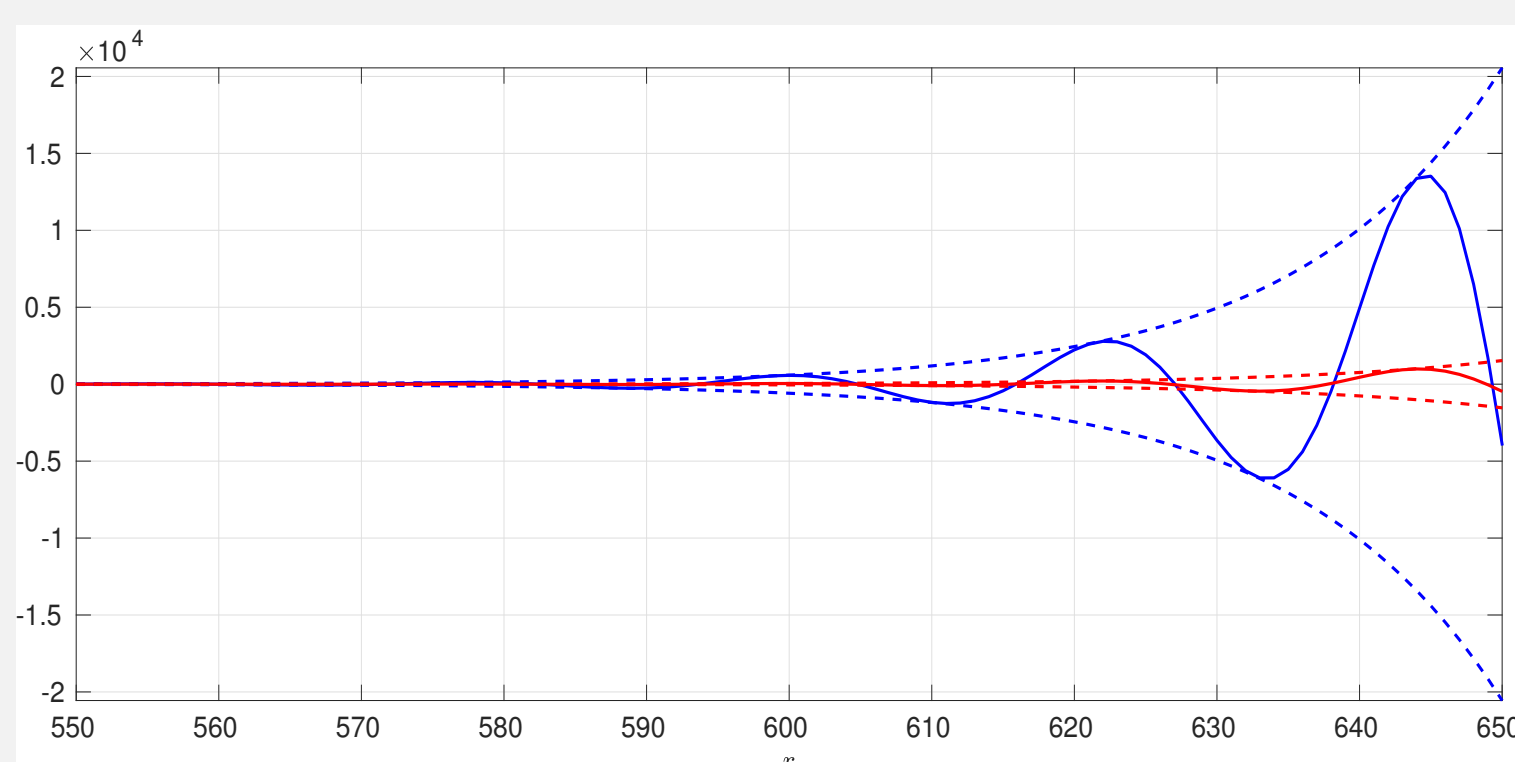


Comparison between critical values of  $R$  for  $U_w = 0.1$  (—) and  $U_w = 0.2$  (---) for stationary disturbances across a range of  $\varphi$ .

- There is a somewhat **optimum** range of  $\varphi$  for which stabilisation is maximised.
- This phenomenon is as yet **unexplained**.

#### Direct numerical simulations:

- Track **radial evolution** of stationary disturbance via time-marching procedure.



Comparison between steady (—) and  $U_w = 0.2$ ,  $\varphi = 16$  (---) radial wavetrains.

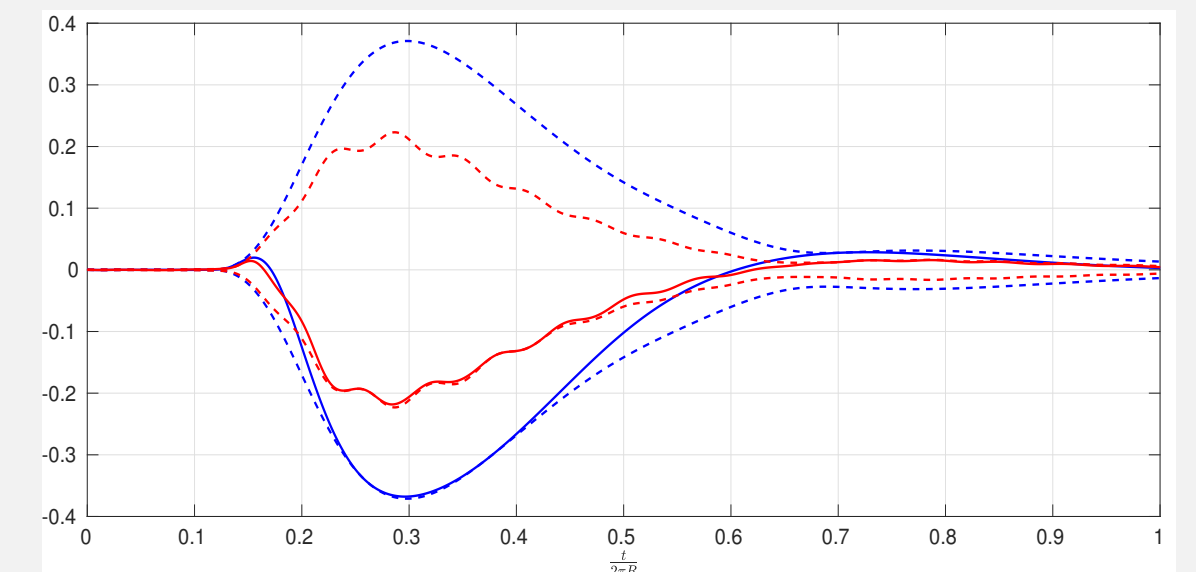
- We see a clear reduction in radial growth rate as expected.

### Impulsive Disturbances

- Specify wall motion of the form (4), centered around some radial location  $r_f$ .
- Track temporal development at **fixed radial location**.
- The rotating disk contains an **absolute instability** for  $R > 507$ ,  $n \approx 68$  [3].
- Thus, for these parameter values, any disturbance will **grow at all radial locations for all times**.

#### Convective instability:

- The following figure shows a comparison between the temporal development at a fixed radial location of an impulsive disturbance centered at the convectively unstable parameter values  $R = r_f = 500$  and  $n = 32$ .

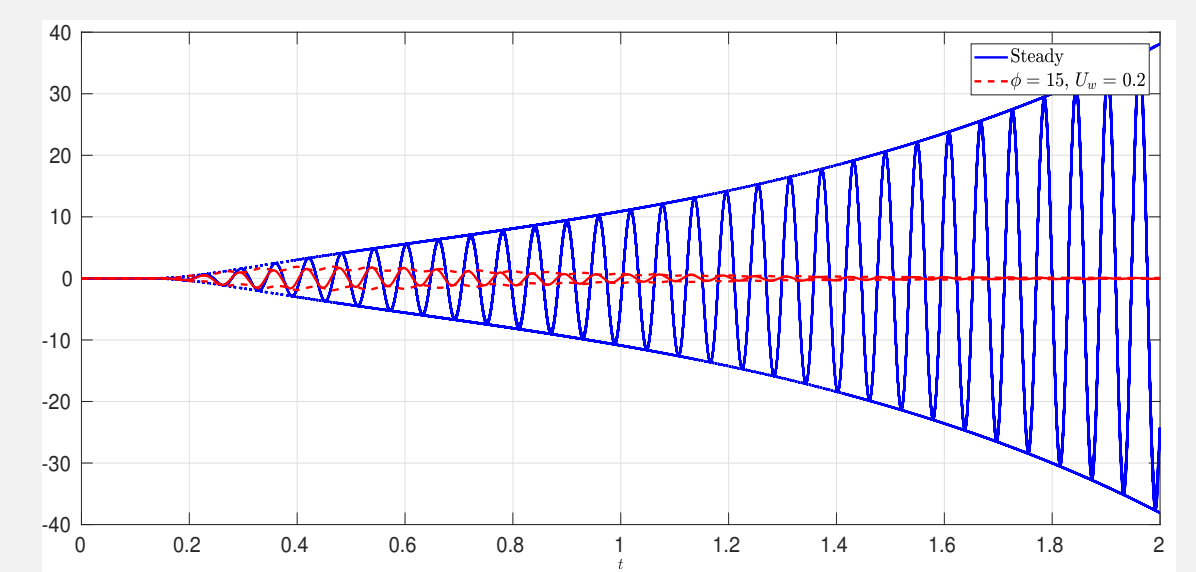


Comparison between steady (—) and  $U_w = 0.2$ ,  $\varphi = 16$  (---) temporal development measured at radial location  $r = 550$  for an impulsive forcing centered at  $R = r_f = 500$  with  $n = 32$ .

- A clear reduction in temporal growth rates is visible, which persists across a range of  $\varphi$ .
- This indicates that the stabilisation is much more **robust** than is indicated by the **single temporal mode** study conducted by the analysis of stationary disturbances.

#### Absolute instability:

- The following figure shows a comparison between the temporal development at a fixed radial location of an impulsive disturbance centered at the absolutely unstable parameter values  $R = r_f = 525$  and  $n = 68$ .



Comparison between steady (—) and  $U_w = 0.2$ ,  $\varphi = 16$  (---) temporal development measured at radial location  $r = 600$  for an impulsive forcing centered at  $R = r_f = 550$  with  $n = 68$ .

- Again, a clear reduction in temporal growth rates is visible, which persists across a range of  $\varphi$ .
- This indicates that the absolute instability is also stabilised, and in some cases, for a certain set of parameter values, **eliminated entirely**.

### Future Directions

#### Short-term:

- Conduct more thorough **parametric analysis** to illustrate all aspects of stabilising behaviour.
- Provide plausible **physical explanations** for modulation effects.
- Study parallels between temporal modulation and periodic surface roughness, which is of particular interest to the aerospace industry.

#### Long-term:

- Study **torsional oscillations** of the disk surface.
- Explore connections with **hydrodynamic voltammetry at rotating and rocking disk electrodes**.

### References

- [1] THOMAS, C., BASSOM, A., BLENNERHASSETT, P. & DAVIES, C. 2010 The linear stability of oscillatory Poiseuille flow in channels and pipes *Proc. R. Soc.* **467**, 2643-2662.
- [2] DAVIES, C. & CARPENTER, P. W. 2001 A novel velocity-vorticity formulation of the Navier-Stokes equations with applications to boundary layer disturbance evolution. *J. Comput. Phys.* **172**, 119-165.
- [3] LINGWOOD, R. J. 1995 Absolute instability of the boundary layer on a rotating disk. *J. Fluid Mech.* **299**, 17-33.